Journal of Structural Geology 30 (2008) 963–975

Contents lists available at ScienceDirect

Journal of Structural Geology

journal homepage: www.elsevier.com/locate/jsg

Neo-Alpine structural evolution and present-day tectonic activity of the eastern Southern Alps: The case of the Ravne Fault, NW Slovenia

V. Kastelic [a,*], M. Vrabec [a], D. Cunningham [b], A. Gosar [c]

[a] Department of Geology, Faculty of Natural Sciences and Engineering, University of Ljubljana, Askerceva 12, 1000 Ljubljana, Slovenia
[b] Department of Geology, University of Leicester, Leicester, UK
[c] Seismology and Geology Office, Environmental Agency of the Republic of Slovenia, Ljubljana, Slovenia

ARTICLE INFO

Article history:
Received 31 May 2007
Received in revised form 5 March 2008
Accepted 27 March 2008
Available online 8 April 2008

Keywords:
Eastern Southern Alps
Geometry of fault zone
Fault reactivation
Strike-slip faulting

ABSTRACT

The Ravne Fault is an actively propagating NW–SE trending dextral strike-slip fault in the Julian Alps of NW Slovenia, which has been responsible for two moderate sized earthquakes in the last decade. Strike-slip displacements on moderate-steep fault planes are responsible for the recent seismic activity that is confined to shallow crustal levels. The fault is growing by interaction of individual right stepping fault segments and breaching of local transtensional step-over zones. The fault geometry is controlled by the original geometry of the NW–SE trending thrust zone, modified by successive faulting within the fault zone. In the modern N directed maximum horizontal stress regime, the segmented fault is lengthening by active growth at the fault's NW end. The spatial distribution of earthquake clusters shows that activity on strike-slip segments and thrust faults is contemporaneous. Detailed analysis of the spatial pattern of earthquake events and surface fault geometries suggests that for earthquakes of similar magnitudes and similar fault kinematics, the deciding factor for whether an earthquake rupture will breach a step-over zone is the relationship between the lengths of individual neighbouring fault segments and fault separation distances in the step-over-zones. The Ravne Fault represents an example of a tectonic structure that lies in an area subjected to multiple tectonic events under different regional stress conditions. At epicentral depths, the fault system is accommodating recent strain along newly formed fault planes, whereas in upper parts of the crust the activity is distributed over a wider deformation zone that includes reactivated brittle thrust faults.

1. Introduction

The Southern Alps represent a south to southwest vergent part of the Alpine orogen that originated by Tertiary polyphase collisional and post-collisional contractional deformation, associated with continuous northward movement of the Adriatic microplate against the Eurasian plate. Western Slovenia is an actively deforming region at the NE corner of the Adria–Eurasia collision zone, where the plate boundary changes orientation from NW–SE to E–W (Fig. 1). Geographically, this region includes the Julian Alps in the NW part of Slovenia and their western continuation, the Friuli Alps in neighbouring NE Italy (Fig. 1). The structural geology of the transition zone between the Southern Alps and Dinaride chain is complex. There is a gradual change in the geometry and kinematics of recent deformation from south directed thrusting in the Friuli Alps to oblique and predominantly dextral strike-slip deformation in western Slovenia, indicated by earthquake and structural data. This transition reflects the influence of the curved boundary of the Adria indentor on the local deformation field.

The Julian Alps have been subjected to multiple tectonic phases since the Eocene, leading to development of structures with variable orientations and kinematic histories and therefore variable potential for reactivation under modern stress conditions. The fault system analysed in this study is the NW–SE trending Ravne Fault, which cuts through the South Alpine thrust unit along its NW and central lengths (Fig. 1). The active deformation along the Ravne Fault zone is concentrated in the upper parts of the crust, which is characterised by a high density of older structural elements such as fault planes, fractures and cleavage, which represent planes of mechanical weakness. The Ravne Fault presents an important case study of how strike-slip faults initiate, propagate and grow through incorporation of reactivated fault segments within an older thrust stack. The Ravne Fault also presents a unique opportunity to document the along-strike and down-dip geometry of the segmented fault system because it cuts mountainous terrain with more than 1400 m of topographic relief along its length.

In 1998 and 2004, two earthquakes occurred within the Ravne Fault zone. The spatial coverage of both events and their aftershock

* Corresponding author. Fax: +386 14704 560.
E-mail address: vanja.kastelic@ntf.uni-lj.si (V. Kastelic).

0191-8141/$ – see front matter © 2008 Elsevier Ltd. All rights reserved.
doi:10.1016/j.jsg.2008.03.009

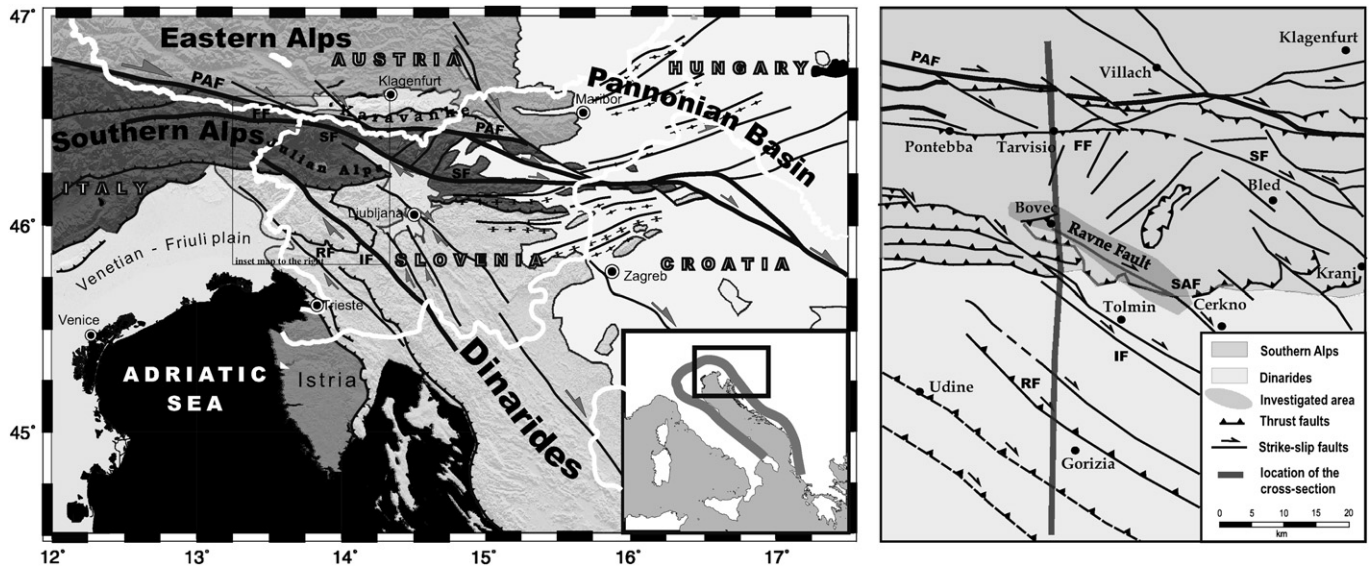

Fig. 1. Regional tectonic framework of Slovenia and neighbouring regions. PAF (Periadriatic Fault), FF (Fella fault), SF (Sava Fault), SAF (South Alpine thrust front), IF (Idrija Fault), RF (Raša Fault). The thick line in small inset represents assumed position of the Adria microplate boundary. The figure on the right shows major faults in the eastern Southern Alps and NW part of the Dinarides. The shaded part of the figure represents the area that was covered by detailed mapping. The line represents the location of the profile shown in Fig. 2.

sequence is very good (Bajc et al., 2001) and allows for accurate determination of fault plane locations and establishment of focal mechanisms to be used to constrain kinematic models of active deformation.

In this paper, we present detailed structural data on the geometry and kinematics of the Ravne Fault together with analysis of the spatial distribution of earthquake clusters and focal mechanisms for the 1998 and 2004 Ravne Fault earthquakes. Our objective is to better understand processes of active strike-slip fault propagation in crust that contains pre-existing thrust faults. The multidisciplinary approach of our research allows comparison of the deep and shallow architecture of the Ravne Fault and demonstrates how detailed earthquake data can lead to a better understanding of the spatial distribution and kinematics of recent fault motions.

2. Regional structural setting

The domain of active strike-slip deformation in NW and W Slovenia is positioned between the S vergent thrust domain in the Friuli area of NE Italy and SW thrusting domain of the Dinarides. Earthquake data in NE Italy indicate that the prevailing mechanism of deformation is thrusting on E–W oriented planes whereas dextral-reverse and purely dextral strike-slip displacements on NNW–SSE oriented planes occur further E and SE (Vannucci and Gasperini, 2004). The prevailing fault orientation in the Dinarides is in the orogen-parallel NW–SE direction. Earthquakes along these faults exhibit thrust focal mechanisms in the southern and central parts of the Dinarides, and dextral-reverse mechanisms in the northern Dinarides bordering our study area (Herak et al., 1995; Poljak et al., 2000; Ivančić et al., 2006).

The first stage of mountain building connected to the South Alpine orogeny is Eocene thrusting and reverse fault movements along the NE Adriatic margin. During the Eocene to Lower Miocene, NE–SW directed shortening led to thrusting and uplift along SW vergent NW–SE oriented faults in the Central and External Dinarides (e.g. Tari and Pamić, 1998; Pamić et al., 2002), Julian and Friuli Alps, and E Dolomites (Doglioni, 1987; Table 1). Palaeostress calculations suggest that this deformation was driven by 025° to 055° SH_{max} directed compression (Castellarin and Cantelli, 2000). The Eocene Dinaric faults were strongly dismembered by younger, mostly late Oligocene and Miocene, south-vergent South-Alpine thrusts (Fig. 2) and steep reverse faults, which resulted in overthrusting and refolding of Dinaric structures both in the Friuli region (Doglioni, 1987; Nussbaum, 2000) and in the Julian Alps (Placer and Čar, 1998). During Late Oligocene–Miocene South Alpine shortening, the orientation of the maximum compressive stress within the entire region was on average NNW–SSE (340°; Castellarin and Cantelli, 2000), which resulted in formation of E–W oriented thrust and reverse faults. This south to southeast vergent fold and thrust belt was formed as a late stage retro-wedge of the Alpine collision, probably due to indentation of Adriatic lower crust into European lithosphere (Schmid et al., 1996; TRANSALP Working Group, 2002; Brückl et al., 2007).

During the Miocene–Pliocene transition, the Alpine region was subjected to a change in regional style of deformation probably due to termination of subduction and slab pull along the eastern edge of the Carpathians (Horváth and Cloetingh, 1996). This change in the regional stress field coupled with the continuous northward motion of Adria resulted in widespread inversion of extensional structures in the Pannonian basin units (Fodor et al., 1998) and counter-clockwise (CCW) rotation of Adria (Márton et al., 2002). In

Table 1
Simplified description of tectonic phases from Eocene to recent, for the eastern Southern Alps (further explanation in the text)

Name of tectonic phase	Dinaric thrusting	South-Alpine thrusting	Strike-slip activity
Period of activity	Eocene	Oligocene–Miocene	Pliocene–recent
Orientation of main stress axis	N55°–N25° (Castellarin and Cantelli, 2000)	N340° (Castellarin and Cantelli, 2000)	N–S (Grenerczy et al., 2005)
Fault activity	Thrusting/reverse faulting on NW–SE oriented fault planes	Thrusting on E–W oriented fault planes	Dextral strike-slip movements on NW–SE oriented faults

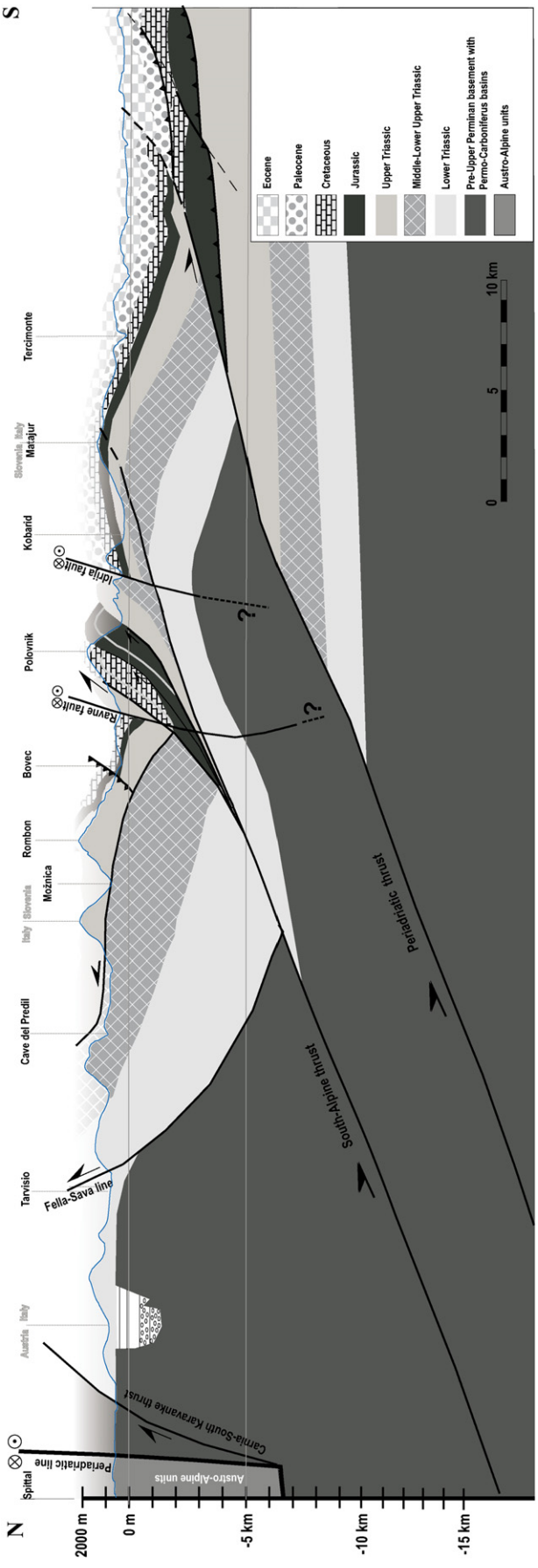

Fig. 2. N–S profile across the western part of the Julian Alps from the Periadriatic fault to the Friuli plain. Data from the TRANSALP deep seismic profile (Lüschen et al., 2006) were used to construct the deeper parts of the section. Fault geometry data from the neighbouring Friuli Alps (Nusbaum, 2000) were used to better constrain and correlate the structures. Location of transect shown in Fig. 1.

the Julian Alps, oblique convergence along the NE boundary of the Adria plate probably led to the initiation of dextral strike-slip faulting on NW–SE trending steep faults (Vrabec and Fodor, 2006). The ongoing deformation in Slovenia is driven by the northward push of Adria against Europe and continued CCW rotation of the Adria microplate. Directions of active crustal displacements based on a calculated Euler pole retrieved from GPS data indicate N–S shortening at 2 mm/yr (Grenerczy, 2002; Weber et al., 2006).

3. Regional seismicity

The western Julian Alps together with the Friuli-Venezia Giulia region of NE Italy is the most seismically active area in the entire Alpine region. The seismicity in the eastern Southern Alps shows that both the south-vergent Alpine thrusts and the NW–SE trending Dinaric faults are active within the same stress field. Focal mechanisms indicate the average N–S orientation of the maximum compressive stress (Slejko et al., 1999), but there is a clear distinction between the pure N–S orientation in the western and central regions, and more NNE–SSW orientation in the eastern (Bressan et al., 1998) and southeastern region (Bressan et al., 2003).

Fault plane solutions for western Slovenia typically show dextral-strike slip to dextral-reverse kinematics on steep NE dipping fault planes (data in Renner and Slejko, 1994; Poljak et al., 2000). The strongest earthquake recorded in the region was the 1511 western Slovenia $M = 6.8$ earthquake for which the exact location and mechanism are still debated, although it is believed to have occurred along one of the parallel NW trending faults of W Slovenia, most probably the Idrija Fault (Fig. 1; Fitzko et al., 2005). Other strong historic earthquakes recorded in the region include the 1976 Friuli seismic sequence. According to field data and recent relocations of seismic events (Pondrelli et al., 2001), the 1976 Friuli seismic sequence is E–W oriented with the majority of strong aftershocks occurring along north dipping thrust planes within shallow crustal levels (Anderson and Jackson, 1987). Individual aftershocks, whose epicentres lie more to the SE, indicate moderate dipping, NW–SE oriented fault planes and a single aftershock late in the sequence demonstrates dextral strike-slip movement on a NNW–SSE oriented fault (Pondrelli et al., 2001). In 1998 and 2004 two medium-sized earthquakes struck NW Slovenia. Both seismic events were confined to the upper 10 km of the crust and reached $M_W = 5.6$ (Bajc et al., 2001) and $M_W = 5.2$ (Živčić and Krn-2004 team, 2006) respectively. The focal mechanisms for both earthquakes show almost pure dextral strike-slip (Zupančič et al., 2001; Kastelic et al., 2006).

Besides stronger instrumentally recorded earthquakes, moderate size earthquakes and earthquake clusters are frequent in the region of the eastern Southern Alps. Among the stronger events are the January to June 1996 Claut swarm with recorded $M_L = 4.5$, the 1998 Trasaghis $M_L = 4.0$ event, and the 2002 $M_L = 5.1$ Mte. Sernio earthquake with epicentres in Friuli (Franceschina et al., 2006). In 2005, the $M_L = 4.0$ Bohinj ridge earthquake occurred in the Julian Alps in Slovenia (Živčić, 2005).

Within the structural unit of the Dinarides, two fault zones exhibit seismic activity. Although the Idrija fault is the most obvious fault in the region, instrumental and macroseismic events along its length are scarce. Apart from the presumption that the 1511 earthquake occurred on the Idrija Fault, only two other earthquakes of moderate size have been documented from the system. These are the 1926, $M = 5.8$ event that occurred on the SE part of the fault and the $M = 3.9$, 1983 (Živčić, 2005) event occurring at the NW end of the fault in the border zone with Italy. In addition, the Raša Fault, a NW–SE trending fault zone, situated directly SW of the Idrija fault, is seismically active (Fig. 1). The seismicity on this fault is concentrated at its SE part around Ilirska Bistrica, close to the border with Croatia. The strongest event recorded within this area is the 1916,

$M = 5.8$ earthquake (Kuk et al., 2000) whereas moderate seismic activity is frequently recorded along the fault zone (Ribarič, 1994; Živčić, 2005).

4. Ravne Fault data

The surface trace of the Ravne Fault can be observed in the field and on satellite and digital topographic imagery over a distance of approximately 30 km in a NW–SE direction between Kal Koritnica (Fig. 3) in the NW and Cerkno (Fig. 1) at the SE end. We define the surface trace as the course of the actual fault plane, which is visible in some parts, whereas in other parts, it is indicated at the surface by increased fracturing and erosional incision as a consequence of deeper fault-movements. At the NW end of the surface trace, there are several parallel NW–SE oriented rock-walls a few tens of metres in length and height that could indicate the presence of a fault, but any more tangible evidence for surface fault activity is absent. At the SE end of the fault trace towards the Cerkno area, the surface expression of the fault trace is progressively less visible and eventually dies out. However, according to the 1:100.000 geological map of the area, a NW striking reverse/thrust continues towards the SE from that area (Grad and Ferjančič, 1968). The fault is best exposed in its central part around the Tolminka Springs basin over a length of approximately 11 km from the Čez Potoče pass in the NW to the Tolminske Ravne in the SE (Fig. 3). Over its total course, the fault cuts through very diverse topography with relief in excess of 1400 m from lower elevations at 450 m to high mountainous terrain up to 1860 m elevation, including the Krn mountain chain (Fig. 3).

The surface trace of the Ravne Fault was analysed and mapped in the field. Where exposed, fault planes were mapped in detail, taking into account lateral and vertical changes in fault plane orientations. The orientation of sedimentary bedding of Upper Triassic limestone bedrock and other secondary structures in fault wall rocks were also measured to assess their relationship to the main Ravne Fault structure. Kinematic indicators such as calcite mineral steps, dragged layering in adjacent cataclastic rocks, and the orientations of Riedel shears and subordinate splays adjacent to the trace of the main fault plane were analysed to determine sense of movement. In areas of lesser exposure, more consideration was given to geomorphic features to identify the trace of the fault, including local depressions along the length of the fault trace, presence of saddles on ridges, and areas of river incision. Detailed maps of the topographic expression of faulting in the Tolminka Springs basin area were also created using airborne LiDAR and digital relief models, which were later ground verified (Cunningham et al., 2006).

An important observation along the trace of the Ravne Fault is the relationship between the dip direction of sedimentary bedding and fault geometry. Along the fault trace from Planina Predolina to Tolminka Springs basin, the rocks on the SW side of the fault dip towards the NNE or NE—towards the fault. On the contrary, on the NE side of the fault and roughly in the same area, the dip of sedimentary layers of the same stratigraphy is towards the SSW or SW—again towards the trace of the fault. Fig. 4 shows orientation of bedding as well as faults and fractures depicted in equal area lower hemisphere stereoplots near the trace of the Ravne Fault and the orientation of thrust fault planes.

4.1. Segmentation model

Fault segmentation may result from initial development of the fault as separate en echelon segments, linkage of pre-existing unconnected structures, or from the breakdown of a larger pre-existing structure (Vermilye and Scholz, 1999). Field mapping revealed that the Ravne Fault exhibits a segmented geometry along

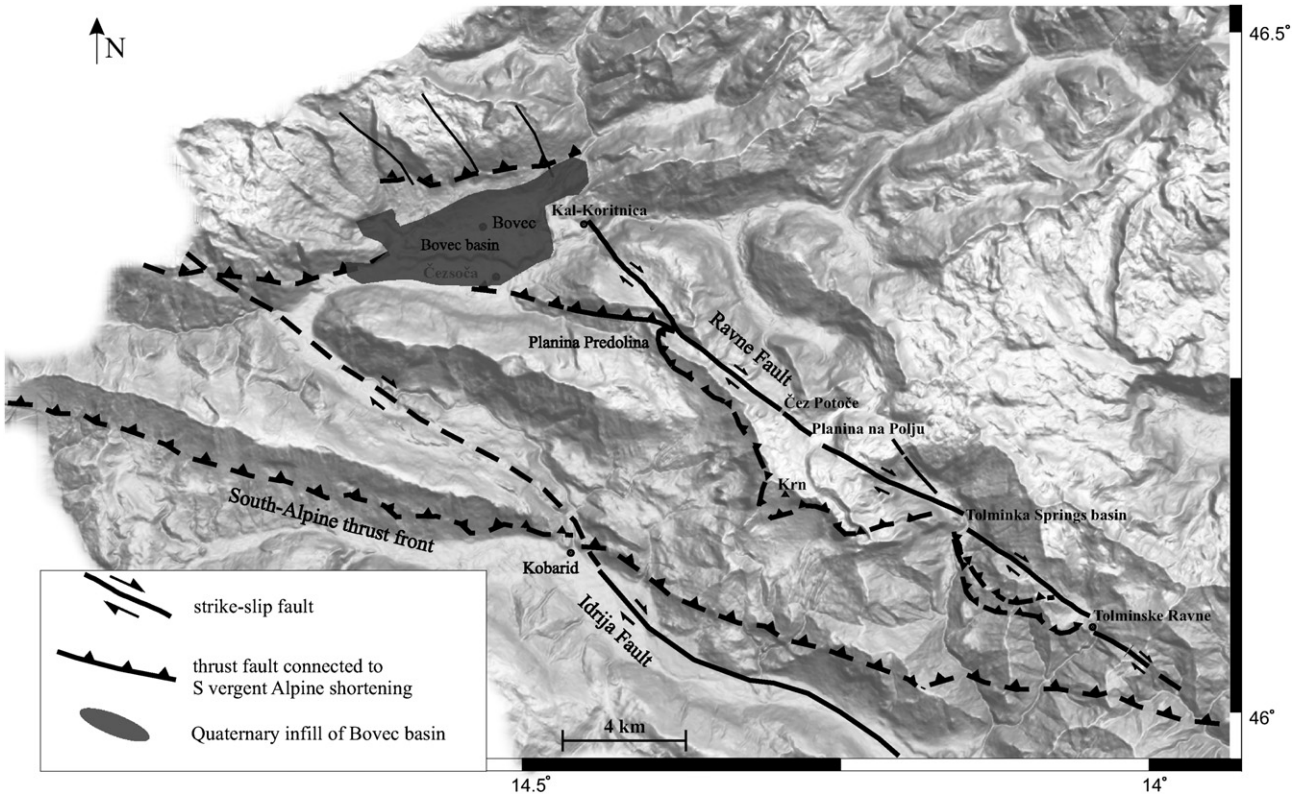

Fig. 3. Main faults in NW Slovenia shown on a DEM illuminated from the NE. The Ravne Fault exhibits a right-stepping geometry with local transtensional basins of Planina na Polju, Tolminka Springs basin and Tolminske Ravne located in step-over zones.

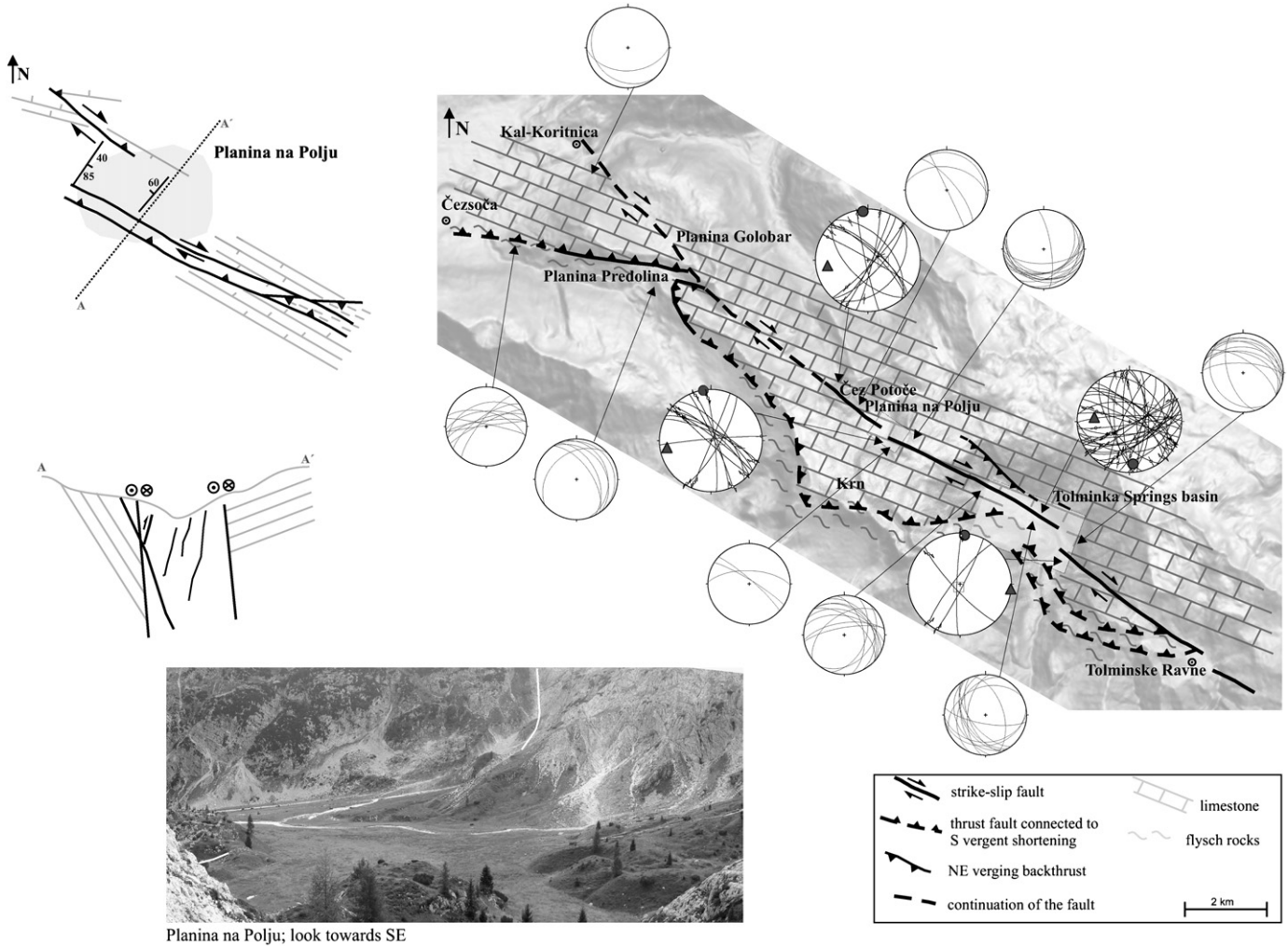

Fig. 4. Geometry of Ravne Fault zone and associated structures in a transect from Kal Koritnica to Tolminske Ravne with the structure of the Planina na Polju area shown in more detail (position of Planina na Polju area along the trace of Ravne Fault is shown with a small rectangle). Small stereoplots show the orientation of bedding along the mapped fault trace. Large stereoplots show orientation of fault and fracture planes within the fault zone. Circles and triangles within the stereoplots indicate orientation of maximum and minimum stress axis, respectively, determined by inversion of fault-slip data. The rectangular area around the Tolminka Springs basin shows the location of the Fig. 5.

its trace (Fig. 4). Overall, the fault is arranged in a right-stepping manner as four fault segments of different lengths with slight variations in NW strike. Towards the NW end of the trace, where there is progressively less exposure, the first segment was identified between Čez Potoče pass and Planina na Polju with a length of 1.1 km. At Planina na Polju, this segment overlaps with a 4.2 km long segment that stretches from Planina na Polju to Tolminka Springs basin. The two fault segments overlap over a length of 425 m and the separation between them is 80 m. Due to the right-stepping arrangement of fault segments along a right-lateral fault zone, a small transtensional basin 500 m in length (NW–SE direction) and 450 m in width (NE–SW direction) formed at Planina na Polju (Fig. 4). Exposure in this part of the fault zone is good. Several fault planes were recognised with dominantly moderate NE–NNE dips. Toward the end of each segment, the deformation zone widens and an array of parallel and sub-parallel to oblique small fault planes and fractures can be observed. Close to the region where both segments start to overlap, evidence of transtensional normal faulting, including lowered hanging wall blocks and triangular fronted surfaces occur. The lowering of hanging-wall blocks is evident on SE dipping normal fault planes on the NW side, as well as on NW dipping planes at the SE end of the basin. Both segments run in narrow gullies through otherwise mountainous terrain, forming a distinctive landscape feature. Fault gouge a few centimetres in width can be observed along individual fault planes, and fine-grained breccias of wall rock and a high degree of rock damage are evident close to and in the overlap zone. Besides the shattered aspect of the limestones cropping out along the fault trace, evidence of secondary dolomitisation is extensive in the overlap region.

In the area of the Tolminka Springs basin, the fault segment running SE of Planina na Polju overlaps in a right-stepping manner with a NW–SE oriented, 5.9 km long segment that ends at Tolminske Ravne towards the SE (Fig. 5). As in the case of Planina na Polju, this also is an elongate transtensional basin 2.1 km long in a NW–SE direction and 510 m wide in a NE–SW direction. The two main Ravne Fault segments that enter the Tolminka Springs basin overlap by 370 m and are separated by 300 m. The Tolminka Springs basin forms an obvious geomorphic step in the local topography as it represents 1200 m of terrain lowering. Such relief is the consequence of both tectonic lowering as well as intense erosional processes caused by massive landsliding, which is responsible for volumetrically large debris cones in the NW and NE part of the basin. Evidence for strike-slip and oblique-slip movements is confined to exposures in narrow gullies which mark the eroded fault zone, whereas within the overstep region, no actual

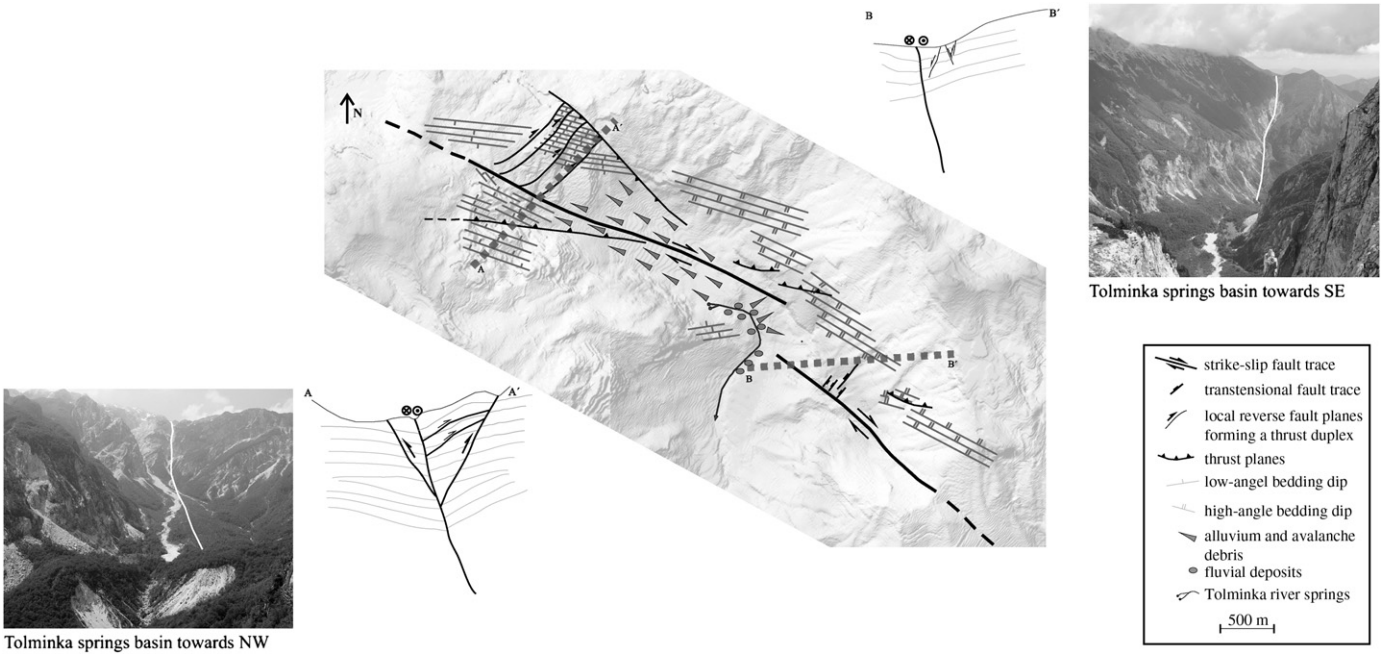

Fig. 5. Geometry of Ravne Fault zone in the Tolminka Springs basin. The photo in the left part of the figure shows a thrust duplex connected to NE–SW directed shortening., In the front of the photo, incision of Tolminka River into unconsolidated alluvial and avalanche sediments is clearly visible. The photo on the right side shows the area of interaction between two NW–SE oriented fault segments that was not breached by recent seismic events. In both photos the white line represents the trace of NW–SE striking strike-slip faults. The location of the Tolminka Springs basin along the trace of the Ravne Fault is shown in Figs. 3 and 4.

fault planes are observed at the surface due to cover of coarse sediments. Close to and in the area of overlap, transtensional normal faulting is suggested by topographic steps and cliffs that appear to be degraded scarps of NNE–SSW and NW–SE trending faults, but again due to erosion and sediment accumulation, the fault planes are not exposed. The name Tolminka Springs basin comes from two springs under the mountain near the SW side of the basin that form the source of the Tolminka River that drains the area. Within 300 m of the actual springs, the river cuts a 100-m deep channel through alluvial and avalanche material. This may suggest that the wider area is actively uplifting as the response of a river system to uplift is to cut down to retain its base level (Keller and Pinter, 1996).

The Ravne fault is less exposed to the SE of the Tolminka Springs basin, where it is covered by grass and forested terrain. The fault trace between the Tolminka Springs basin and areas SE of Tolminske Ravne is still marked by narrow gullies, but no individual fault planes outcrop. Along that part of the fault trace, the fault again exhibits a right-stepping fault segmentation pattern and both segments overstep in the area of Tolminske Ravne (Fig. 3). The determined length of the fault segment SE of Tolminske Ravne is only 950 m as surface continuation of the fault to the SE is difficult to discern and therefore uncertain.

4.2. Fault growth

Faults grow by repetitive cycles of tip-line propagation, overlap and linkage of smaller faults (e.g. Peacock and Sanderson, 1991, 1996; Dawers and Anders, 1995; Gupta and Scholz, 2000; Mansfield and Cartwright, 2001). They obey scaling laws related to the overall displacement along their traces and their total lengths (e.g. Schlische et al., 1996). The recent seismic activity of the Ravne Fault did not produce any surface rupturing, but the 1998 earthquake did rupture the fault over a length of 12 km at a depth between 3 and 9 km (Bajc et al., 2001). As the Ravne Fault is comprised of interacting segments, the displacement produced by an earthquake would be asymmetrically distributed along the length of the fault with the maximum displacement on an individual fault segment being shifted towards the interacting tip (Peacock and Sanderson, 1991; Gupta and Scholz, 2000; Scholz and Gupta, 2000; Kim and Sanderson, 2005). The epicentre of the 1998 earthquake is located towards the NW end of the aftershock cluster, suggesting that the NW tip of the fault is actively propagating in the direction of the Bovec basin (Fig. 6). This idea is consistent with the breaching of the Planina na Polju overstep, indicating that fault segments in that area grew to the point of soft-linkage and could also display hard-linkage at depth.

Relationships between displacement (D) and fault length (L), as well as separation (S) and overstep (O) lengths also govern the process of fault growth. Different scaling relations for the D–L relationship have been proposed. Generally the D–L dependence takes the form of $D = L^n$, where the exponent value n ranges from 0.5 to 2.0 (e.g. Cowie and Scholz, 1992; Dawers et al., 1993; Scholz et al., 1993; Kim and Sanderson, 2005 and references therein). According to some studies (Gupta and Scholz, 2000), separation-overlap values can distinguish between interacting and non-interacting fault segments when normalised to the fault length. The ratio between 10% of the total fault length and the distance of mutual separation between adjacent segments governs the possibility of fault interaction for strike-slip faults (An, 1997). The 80 m stepover separation and 425 m overlap length for parallel fault segments at Planina na Polju could therefore be easily breached by a seismic event. A 300 m separation and 370 m overlap length for parallel fault segments in the Tolminka Springs basin can, compared to the length of each segment, experience linkage. The separation–overlap ratio on its own however, suggests that the overlap zone is unfavourable for being breached. For the 1998 earthquake sequence, the aftershocks stopped at the Tolminka Springs overstep zone (Fig. 6) indicating that these particular fault segments do not demonstrate linkage and behave as two separate fault traces. The aftershocks of the 1998 earthquake sequence are distributed along two NW–SE trending fault segments and they stop around the

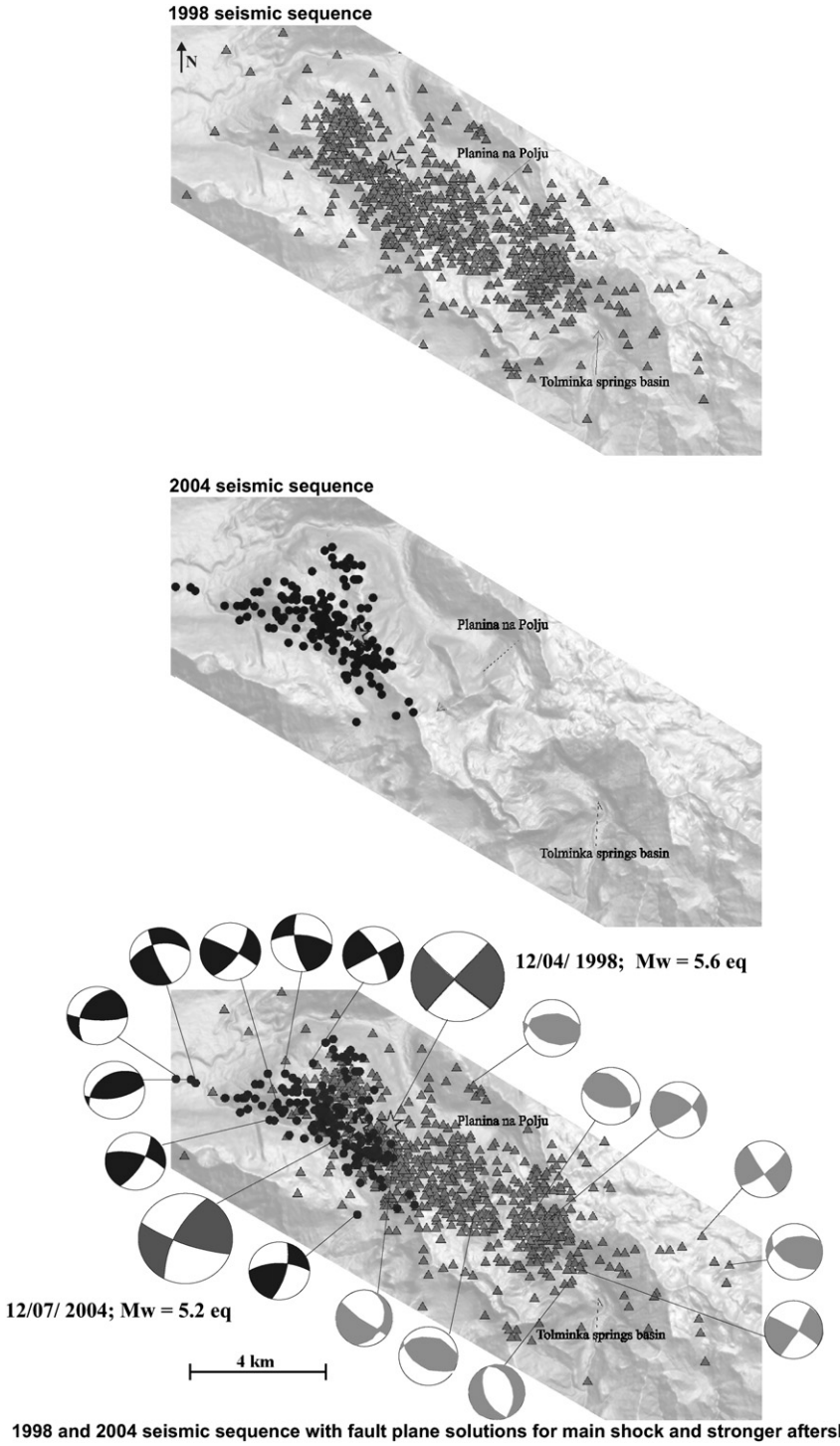

Fig. 6. Spatial distribution of aftershock sequences of the 1998 and 2004 Ravne Fault earthquake events, with focal mechanisms computed for both main shocks and stronger aftershocks. Grey triangles depict the 1998 $M_W = 5.6$ earthquake seismic sequence (Bajc et al., 2001), while the location of the 2004 $M_W = 5.2$ earthquake seismic sequence (Živčič et al., 2006) is shown in black circles. The grey and light-greyish stars represent the 1998 and 2004 main shock locations respectively. The grey-coloured focal mechanism solutions belong to the 1998 aftershock cluster (Zupančič et al., 2001), the black solutions to the 2004 event (Kastelic et al., 2006).

overlap zone of the third segment. The aftershocks breached the overstep zone of Planina na Polju, but the rupturing stopped on the outskirts of the Tolminka Springs basin overstep zone. Two fault systems were involved in faulting as proven by the 2004 earthquake sequence. Part of the seismic activity was distributed on NW–SE trending faults, while a branch of aftershocks was distributed in an E–W direction from the epicentre of the main shock on fault planes with E–W orientation. Near the area where both aftershock clusters are separated, the faults along which the aftershocks are distributed are less than 500 m from each other at the ground surface (Fig. 6). These data support the idea that fault growth is dependent on the unique history of linkage between each individual fault segment (Mansfield and Cartwright, 2001).

4.3. Evolution of the fault zone

In the Ravne Fault zone NE dipping fault planes are abundant (Fig 7). They do not form a single through-going plane, but rather

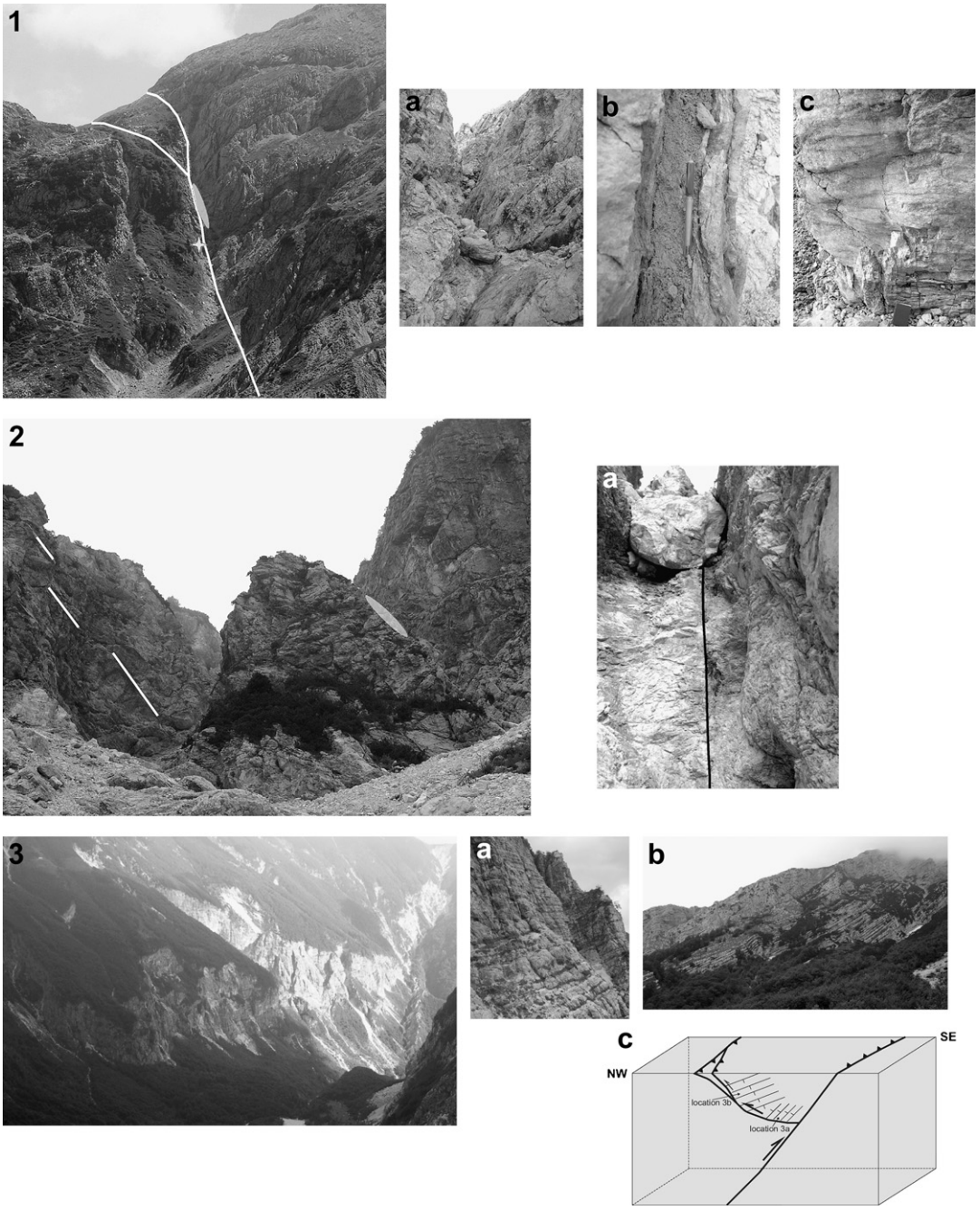

Fig. 7. Ravne Fault exposures. (1) View of the fault gully to the SE from Planina na Polju. Trace of the fault is marked in white. The gully formed along individual NE dipping shear planes (1a) that continue in the S slope, while the main fault trace runs across the high area NW from Tolminka Springs basin. Ellipse shows the position of the fault trace exposure within the gully. The star depicts position of a sub-vertical plane with horizontal grooves (mullions) indicating strike slip displacement (1c). Photo 1b) shows the inner fault cataclastic zone of a moderate NE dipping fault. (2) Exposure at the NW end of Tolminka Springs basin. White lines show locations of individual sheared NE dipping planes. The ellipse in the gully indicates the position of a sub-vertical closed fracture plane which is shown in 2a in a black line. (3) Limestones outcropping at N walls of Tolminka Springs basin dip sub-horizontally to the N (3a), whereas beds in the middle and upper slopes show moderate to steep dips towards SW (3b). This structure is connected to a backthrust of the main NE dipping thrust plane (3c).

consist of individual planes along strike and dip of the fault zone. Dips of individual planes vary from moderate to steep between 60° and 80°. The best exposures of planes with these orientations can be observed in the part of the fault zone between the NW part of the Tolminka Springs basin and Čez Potoče pass. In the area of Čez Potoče pass a NE dipping fault plane outcrops that has thrusted Upper Triassic limestone over Cretaceous flysch rocks (Fig. 8). In the segment between Planina na Polju and Tolminka Springs basin where the fault trace is marked by a narrow gully, numerous planes with NE dips are present along the trace of the gully as well as in the footwall block. The orientation of the gully varies by up to 40° in its general NW–SE orientation and has developed along individual NE dipping fault planes. The geometry of the planes and shear bands indicate uplift of hanging-wall blocks. Adjacent to some planes, well developed cataclastic zones up to a few centimetres wide are developed, whereas in other places, sheared surfaces of polished tectonic breccia occur in the innermost fault zone. Fault-related deformation is not confined to the gully only; rocks in the S wall of

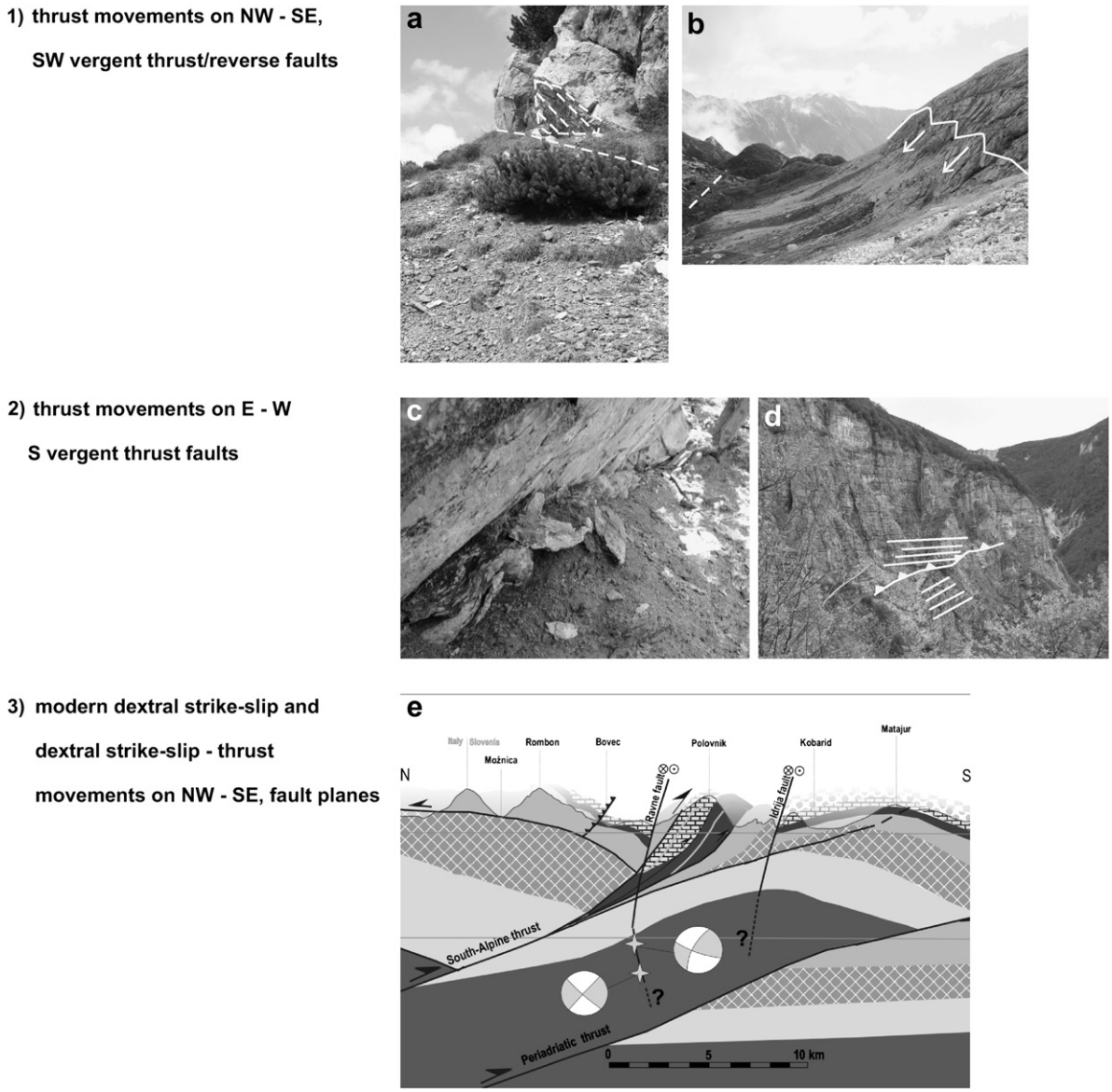

Fig. 8. Structures indicating kinematic history of the Ravne Fault zone. (a) Tectonic contact between Cretaceous flysch rocks in the footwall and Upper Triassic limestone in the hanging wall superposed along a NE dipping thrust plane (dashed area); view towards W. (b) Orientation (full line) and dip (arrows) of tectonic fabric in the Upper Triassic limestone within the footwall of a NW–SE oriented thrust. In the left part of the photo the dashed line represents the trace of a steep-dipping NW–SE oriented strike-slip fault; view towards E. (c, d) NNE dipping thrust planes in the contact between Upper Triassic and Cretaceous rocks. (e) Modern strike-slip activity at epicentral depths on Ravne Fault. Cross-section taken from Fig. 2.

the gully also show a high degree of brittle deformation and NE dipping bedding planes are also sheared.

The same situation can be observed in the higher area situated between Tolminka Springs basin and Planina na Polju where the fault zone is not confined to a gully and no surface exposure of the fault trace is present. A tectonised zone, characterised by sheared NE dipping planes can be observed in a belt several tens of meters in width, running parallel to the strike of the fault zone.

At the NW end of Tolminka Springs basin, a thrust duplex in bedded limestones is exposed, containing four individual SW dipping thrust ramps that indicate NE–SW oriented shortening. Along the N edges of the basin, in the lower parts of the bounding cliffs, outcropping limestones show sub-horizontal to gentle bedding dips to the N, whereas higher up along the ridge summits, beds dip moderately to steeply SW along the entire N edge of the basin and even further to the E and W.

Based on this more regional bedding geometry, we believe that the SW tilted succession of layered Upper Triassic limestone that the Ravne fault cuts through, is backthrusted towards the NE as accompanying deformation on the frontal NE dipping SW-directed thrust plane (Figs. 4 and 7(3c)). This backthrusted sheet forms the peaks and summits of the ridges above the Tolminka Springs basin and represents the phase of the most prominent topography building event within this part of the Julian Alps. The studied part of the Ravne Fault zone lies almost entirely in the South Alpine thrust unit, with the exception of the segment SE of Tolminske Ravne where the fault enters the Dinarides unit (Fig. 1). The border between the two units is a zone of several major E–W trending thrust planes (e.g. Buser, 1986). The position of the thrust zone lies close to the trace of the Ravne fault and in the area of Tolminka Springs basin the thrust zone lies on its southern side. On the N side of the Tolminka Springs basin, minor E–W striking moderate-steep N dipping thrust planes are present. The minor thrust faults lie within layered Upper Triassic limestone and cause a local change of bedding dip in their hanging walls. The dips in the footwall blocks are more northeasterly and are shallower (038°/28°, 040°/16°),

whereas dips in the hanging walls display more northerly and steeper dips (003°/68°, 012°/65°). In the area of Planina Predolina (Fig. 3), an E–W trending, N–NNE dipping thrust fault has superposed Upper Triassic limestones above Cretaceous flysch units. This outcrop is a part of a larger E–W trending thrust plane that stretches from the Planina Predolina area towards the Bovec area to the W. Internally, this unit shows a high degree of deformation with densely developed shear planes oriented parallel to the main thrust plane. Slivers of limestone are present within flysch marlstones and siltstones, but only in the inner thrust zone. Compared to the hanging wall limestones, the flysch rocks are less rigid and have behaved as mechanically weak glide horizons that have preferentially accommodated thrust movements.

Only a few sub-vertical NE dipping (70–80°) planes exhibit slickensides and horizontal grooves and slickenlines within the Ravne Fault. At the NW end of the Tolminka Springs basin, where the trace of the fault is confined to a gully, a sub-vertical NE dipping closed fracture without any visible strike-slip displacement outcrops along the gully, cutting through moderate to steep NE dipping planes (Fig. 7). Therefore, we believe that the sub-vertical planes and fractures are surface precursors of the steeply dipping strike-slip fault zone currently forming at depth, whereas near-surface brittle displacements are predominantly accommodated by older NE dipping thrust/reverse fault planes with shallower dip.

Recent seismic activity recorded in the Ravne Fault zone shows that ongoing seismic activity is confined to shallow crustal levels and does not exceed depths beyond 10 km. The 1998 and 2004 earthquake clusters indicate active dextral strike-slip, oblique dextral-reverse, reverse-dextral to almost pure reverse deformation (Kastelic et al., 2006). The main shocks of both earthquakes delineate almost pure dextral strike-slip movements on steep SW dipping planes (Fig. 6). The 1998 earthquake cluster is distributed in a NW–SE orientation with the main shock located more to the NW end, approximately 4.5 km from the fault's NW end, whereas the SE end of the cluster is at Tolminka Springs basin. Focal mechanism solutions for aftershock events indicate thrust or reverse movements on N dipping fault planes on both ends of the cluster, all within the first 7 km of the crust (Zupančič et al., 2001). The earthquake did not cause surface rupturing, but it did (re)activate a 12 km long and 7 km wide rectangular fault plane with an average slip of 18 cm (Bajc et al., 2001). The 2004 earthquake was weaker and also did not cause surface rupturing. The epicentre of the main shock was located 1 km W of the 1998 epicentre location. This event and its aftershock sequence were also confined to shallow crustal levels. The spatial distribution of aftershocks is not as homogeneous in direction as for the 1998 cluster. Two distinctive branches of aftershocks can be observed for the 2004 sequence; one line continues in a NW–SE direction rupturing an area further NW of the 1998 cluster, while the other line branches off in an E–W direction. The computed focal mechanisms for stronger aftershocks (Kastelic et al., 2006) show similar kinematics as the main shock, the difference being a larger dip-slip component for some

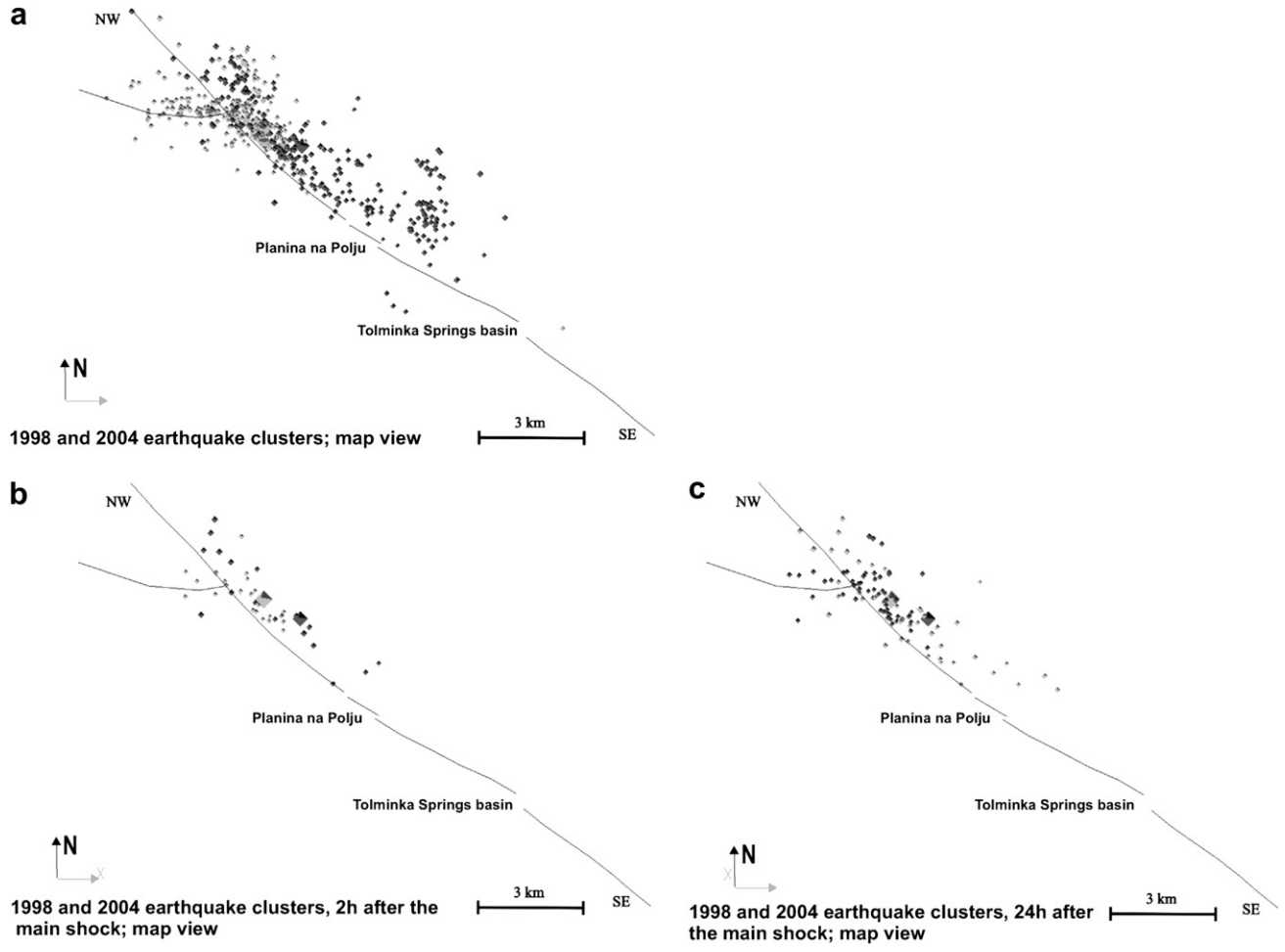

Fig. 9. Spatial distribution of the 1998 and 2004 earthquake clusters. Black tetrahedra stand for location of 1998 aftershocks, grey ones for the 2004 locations. Locations of both main shocks are depicted by larger black and grey tetrahedra for the 1998 and 2004 event, respectively. The smaller size of aftershock tetrahedra shows greater depths of individual events.

aftershocks, indicating oblique dextral-reverse movements on steep to moderate-steep NW–SE oriented fault planes and oblique reverse-dextral and reverse movements on E–W oriented, moderate-steep faults.

4.4. Reactivation model

Existing zones of rheological and mechanical weaknesses play an important role in the geometrical development of newly formed structures in pre-deformed rocks (e.g. Holdsworth et al., 2001; Viola et al., 2004). Old fault planes and fabrics may be favourable candidates for structural reactivation as it is mechanically easier to reactivate pre-deformed planes than to form new ones (Scholz, 1998). At the surface, the Ravne Fault is not a continuous fault plane along its strike, but is an assemblage of individual fault segments, which are older NW–SE trending thrust and reverse faults. The total length of the fault reaches approximately 30 km and the fault exhibits segmented right-stepping geometry. Segmentation of the Ravne Fault is believed to be due to the original geometry of the NE dipping thrust zones and subsequent tectonic events within the region. In the modern stress regime, the fault exhibits strike-slip activity.

The fault plane solutions show that newly forming fault planes at epicentral depths are steeply SW dipping. No planes with such orientation outcrop within the Ravne Fault zone, except for SW dipping planes connected to Dinaric backthrusting that are observable in the N slopes and summits at the NW end of the Tolminka Springs basin.

The spatial distribution of aftershock clusters supports the reactivation history (Fig. 9). The dimensions of co-seismic rupture can be estimated from the aftershock spatial occurrence within the first few hours after the main shock (Wells and Coppersmith, 1994). For reasons of stress redistribution after the main earthquake shock, early aftershocks occur at the perimeter of the co-seismic rupture zone and the central part around the epicentre is characterised by lack of seismicity for the first hours to days after the main shock (Mendoza and Hartzell, 1988). For the 1998 and 2004 earthquake sequence, there is no clustering of aftershocks on the edge of the ruptured plane (Fig. 9). The aftershocks within the first hours after the main earthquake shock, as well as the whole aftershock sequence, are spread across the entire area of the activated plane and also outside of it. Rupturing of newly forming faults is connected to stress surpassing the strength of the host rock, while fault reactivation only needs to breach the friction on a plane. Pre-existing faults/discontinuities are surfaces with lower cohesive strength and friction coefficients with respect to intact rocks (Anderson, 1951) and rocks in the upper part of the crust due to their brittle behaviour preserve older planar discontinuities. The main shocks occurred at 8 and 6 km for the 1998 and 2004 events, respectively. At the deeper parts of the aftershock cluster, single events are distributed in a narrow zone. Towards shallower levels, the earthquake cluster progressively widens and single events are distributed on planes in a zone 6 km wide measured roughly perpendicular to the strike of the fault zone (Fig. 10). Fault plane solutions for aftershocks give dextral-strike slip and oblique movements on steep NE dipping planes and thrusting on moderate to shallow dipping NNE to N dipping planes. So while recent strain at epicentral depths is being accommodated by newly forming steep fault planes, in upper parts the activity is more diffusely distributed over a wider deformation zone including older faults and fractures.

Combined structural and seismological evidence from the Ravne Fault zone indicate strike-slip motion on steep-dipping fault planes at epicentral depths, whereas the deformation within upper parts of the crust is manifested by thrust or oblique-thrust motion on more gently-dipping planes. Our data suggest that most of the deformation in the higher structural level is dominantly accommodated by reactivated Dinaric and South Alpine thrust planes, with the possibility that a lesser part of the deformation is partitioned onto newly forming fault planes within the evolving strike-slip fault system.

Fig. 10. Depth distribution of the 1998 and 2004 earthquake clusters. View towards the NW, perpendicular to the trend of Ravne fault zone. At epicentral depth the fault system is rupturing new, steep SW dipping planes, while in the upper part of the system, deformation is distributed along a wider zone. Strike-slip, oblique-slip and thrust events are distributed on NE and E dipping planes of the upper parts of the crust. Note, focal mechanisms are shown in plan view perspective.

Active Ravne Fault deformation is clearly linked to the geodynamic setting of the area. The N-directed movements of Adria in an area where its NE boundary curves from E–W to NW–SE, drives modern strike- and oblique-slip deformation on pre-existing NW–SE striking faults. In adjacent areas more towards the W in NE Italy, where E–W trending thrusts are present, the recent seismic activity is also distributed along the older pre-existing E–W thrust faults which are favourably oriented for reactivation.

5. Conclusions

Every fault displays its own history and structural characteristics depending among other factors on its geodynamic setting, lithological and rheological differences of host rock units, and presence of pre-existing weakness planes within the zone. When studying characteristics and modern activity of a particular fault zone, these factors need to be considered.

Field mapping of the Ravne Fault zone revealed that the fault does not exhibit a continuous surface trace. Instead, the fault zone at surface is an assemblage of moderate to steep NE dipping fault planes demonstrating thrust/reverse displacements. Evidence for surface strike slip faulting is limited and the presence of subvertical fractures and individual planes with horizontal grooves probably represent surface precursors of upwards-propagating steep surface strike slip faults. Segmentation of the Ravne Fault is interpreted to be controlled by the original geometry of NE dipping

thrust zones, later modified by faulting in the modern stress field. The geometrical relationship between separation and overstep of individual fault segments plays a role in distribution of seismic clusters and their ability to breach a gap between two segments and therefore (re)activate larger portions of the fault plane. This demonstrates the importance of geometrical characteristics of the fault zone, especially in the zone of segment boundaries.

The seismological data indicate that within the same earthquake sequence, both south-directed thrust motions on N–S trending planes and dextral strike-slip motions on steep NW–SE directed fault planes have occurred. Endpoints of strike-slip earthquake ruptures are commonly associated with fault steps or the termini of active fault traces (Wesnousky, 2006). The active seismic processes on the Ravne Fault display the same behaviour: the SE end of the earthquake cluster seized up at a transtensional stepover zone because of its geometrical characteristics and the fault gap was not breached during the earthquake. The epicentres of the 1998 and 2004 events are located in an area of poor surface fault exposure and the NW endpoint of the earthquake cluster is in an area where no surface fault trace is observed. Additionally, the main shocks of both events are shifted to the NW relative to the overall spatial distribution of the aftershock cluster, suggesting that active strike-slip fault propagation is NW directed. Furthermore, the spatial distribution and focal mechanisms of aftershocks suggest reactivation of older structures in the strike-slip tectonic regime.

Acknowledgements

Reviews by G. Viola and F. Neubauer substantially improved the quality of the paper. The authors are indebted to Mladen Živčić and Jurij Bajc for relocated earthquake data. This research has been funded by Slovenain Research Agency (ARRS), project number 3311-03-831656.

References

An, L.J., 1997. Maximum link distance between strike-slip faults: observations and constraints. Pure and Applied Geophysics 150, 19–36.
Anderson, E.M., 1951. The Dynamics of Faulting and Dyke Formation with Applications to Britain. Oliver and Boyd, Edinburgh, 191 pp.
Anderson, H., Jackson, J., 1987. Active tectonics of the Adriatic region. Geophysical Journal of the Royal Astronomical Society 91, 937–983.
Bajc, J., Aoudia, A., Sarao, A., Suhadolc, P., 2001. The Bovec–Krn mountain (Slovenia) earthquake sequence. Geophysical Research Letters 28 (9), 1839–1842.
Bressan, G., Snidarcig, A., Venturini, C., 1998. Present state of tectonic stress of the Friuli area (eastern Southern Alps). Tectonophysics 292, 211–227.
Bressan, G., Bragato, P.L., Venturini, C., 2003. Stress and strain tensors based on focal mechanisms in the seismotectonic framework of the Friuli-Venezia Giulia region (northeastern Italy). Bulletin of Seismological Society of America 93, 1280–1297.
Brückl, E., Bleibenhaus, F., Gosar, A., Grad, M., Guterch, A., Hrubcova, P., Keller, G.R., Majdański, M., Šumanovac, F., Tiira, T., Yliniemi, J., Hegedüs, E., Thybo, H., 2007. Crustal Structure Due to Collisional and Escape Tectonics in the Eastern Alps Region Based on Profiles Alp01 and Alp02 from the Alp 2002 Seismic Experiment. Journal of Geophysical Research 112, B06308, doi:10.1029/2006JB004687.
Buser, S., 1986. Basic geological map of SFR Yugoslavia 1:100 000, Sheet Tolmin and Videm. Zvezni geološki zavod, Beograd.
Castellarin, A., Cantelli, L., 2000. Neo-Alpine evolution of the Southern Eastern Alps. Journal of Geodynamics 30, 251–274.
Cowie, P.A., Scholz, C.H., 1992. Displacement-length scaling relationship for faults: data synthesis and discussion. Journal of Structural Geology 14, 1149–1156.
Cunningham, D., Grebby, S., Tansey, K., Gosar, A., Kastelic, V., 2006. Application of airborne LiDAR to mapping seismogenic faults in forested mountainous terrain, southeastern Alps, Slovenia. Geophysical Research Letters 33, L20308, doi:10.1029/2006GL027014.
Dawers, N.H., Anders, M.H., 1995. Displacement-length scaling and fault linkage. Journal of Structural Geology 17, 607–614.
Dawers, N.H., Anders, M.H., Scholz, C.H., 1993. Growth of normal faults: Displacement-length scaling. Geology 21, 1107–1110.
Doglioni, C., 1987. Tectonics of the Dolomites (Southern Alps Northern Italy). Journal of Strucural Geology 9, 181–193.
Fitzko, F., Suhadolc, P., Aoudia, A., Panza, G.F., 2005. Tectonophysics 404, 77–90.
Fodor, L., Jelen, B., Márton, E., Skaberne, D., Čar, J., Vrabec, M., 1998. Miocene-Pliocene tectonic evolution of the Slovenian Periadriatic Line and surrounding area—implication for Alpine-Carpathian extrusion models. Tectonics 17, 690–709.
Franceschina, G., Kravanja, S., Bressan, G., 2006. Source parameters and scaling relationships in the Friuli-Venezia Giulia (Northeastern Italy) region. Physics of the Earth and Planetary Interiors 154, 148–167.
Gebrande, H., Lüschen, E., Bopp, M., Bleibinhaus, F., Lammerer, B., Oncken, O., Stiller, M., Kummerow, J., Kind, R., Millahn, K., Grassl, H., Neubauer, F., Bertelli, L., Borrini, D., Fantoni, R., Pessina, C., Sella, M., Castellarin, A., Nicolich, R., Mazzotti, A., Bernabini, M., TRANSALP Working Group, 2002. First deep seismic reflection images of the Eastern Alps reveal giant crustal wedges and transcrustal ramps. Geophysical Research Letters 29 (10), 92/1–92/4.
Grad, K., Ferjančič, L., 1968. Basic geological map of SFR Yugoslavia 1:100 000, Explanatory notes for Sheet Tolmin and Videm. Zvezni geološki zavod, Beograd, 67 pp.
Grenerczy, G., Sella, G., Stein, S., Kenyeres, A., 2005. Tectonic implication of the GPS velocity field in the northern Adriatic region. Geophysical Research Letters 32, L16311, doi:10.1029/2005GL022947.
Grenerczy, G., 2002. Tectonic processes in the Eurasian-African plate boundary zone revealed by space geodesy. In: Stein. S., Freymueller, J.T. (Eds.), Plate Boundary Zones. AGU Geodynamics Ser. 30, 67–86.
Gupta, A., Scholz, C.H., 2000. A model of normal fault interaction based on observations and theory. Journal of Structural Geology 22, 865–879.
Herak, M., Herak, D., Markušić, S., 1995. Fault plane solutions for earthquakes (1956–1995) in Croatia and neighbouring regions. Geofizika 12, 43–56.
Holdsworth, R.E., Strachan, R.A., Magloughlin, J.F., Knipe, R.J. (Eds.), 2001. The Nature and Tectonic Significance of Fault Zone Weakening. Geological Society Special Publication, 186.
Horváth, F., Cloetingh, S., 1996. Stress-induced late-stage subsidence anomalies in the Pannonian Basin. Tectonophysics 266, 287–300.
Ivančić, I., Herak, D., Markušić, S., Sović, I., Herak, M., 2006. Seismicity of Croatia in the period 2002-2005. Geofizika 23 (2), 87–103.
Kastelic, V., Živčić, M., Pahor, J., Gosar, A., 2006. Seismotectonic characteristics of the 2004 earthquake in Krn mountains. Potresi v letu 2004, EARS, 78–87.
Keller, E.A., Pinter, N., 1996. Active Tectonics; Earthquakes, Uplift and Landscape. Prentice Hall, New Jersey, 331 pp.
Kim, Y.S., Sanderson, D., 2005. The relationship between displacement and length of faults: a review. Earth-Science Reviews 68, 317–334.
Kuk, V., Prelogović, E., Dragičević, I., 2000. Seismotectonically active zones in the Dinarides. Geologica Croatica 53/2, 295–303.
Mansfield, C., Cartwright, J., 2001. Fault growth by linkage: observations and implications from analogue models. Journal of Structural Geology 23, 745–763.
Márton, E., Fodor, L., Jelen, B., Márton, P., Rifelj, H., Kevric, R., 2002. Miocene to Quaternary deformation in NE Slovenia: complex paleomagnetic and structural study. Journal of Geodynamics 34, 627–651.
Mendoza, C., Hartzell, S.H., 1988. Inversion for Slip distribution using teleseismic P waveforms – North Palm Springs, Borah Peak and Michoacan earthquakes. Bulletin of Seismological Society of America 78, 1092–1111.
Nussbaum, C., 2000. Neogene tectonics and thermal maturity of sediments of the easternmost Southern Alps (Friuli area, Italy). Ph.D thesis, Institute de Géologie Université de Neuchâtel.
Pamić, J., Tomljenović, B., Balen, D., 2002. Geodynamic and petrogenetic evolution of Alpine ophiolites from the central and NW Dinarides: an overview. Lithos 65, 113–142.
Peacock, D.C.P., Sanderson, D.J., 1991. Displacements, segment linkage and relay ramps in normal fault zones. Journal of Structural Geology 13, 721–733.
Peacock, D.C.P., Sanderson, D.J., 1996. Effects of propagation rate on displacement variations along faults. Journal of Structural Geology 18, 311–320.
Placer, L., Čar, J., 1998. Structure of Mt. Blegoš between the Inner and Outer Dinarides (in Slovenian). Geologija 40, 305–323.
Poljak, M., Živčić, M., Zupančič, P., 2000. Seismotectonic characteristics of Slovenia. Pure and Applied Geophysics 157, 37–55.
Pondrelli, S., Ekström, G., Morelli, A., 2001. Seismotectonic re-evaluation of the 1976 Friuli, Italy, seismic sequence. Journal of Seismology 5, 73–83.
Renner, G., Slejko, D., 1994. Some comments on the seismicity of the Adriatic Region. Bolletino di Geofisica Teorica e Applicata 36, 381–398.
Ribarič, V., 1994. Earthquakes in Slovenia (in Slovenian). Slovenska matica, 173 pp.
Schlische, R.W., Young, S.S., Ackermann, R.V., Gupta, A., 1996. Geometry and scaling relations of a population of very small rift-related normal faults. Geology 24, 683–686.
Schmid, S.M., Pfiffner, O.A., Froitzheim, N., Schönborn, G., Kissling, E., 1996. Geophysical geological transect and evolution of the Swiss-Italian Alps. Tectonics 15, 1036–1064.
Scholz, C.H., 1998. Earthquakes and friction laws. Nature 391, 37–42.
Scholz, C.H., Gupta, A., 2000. Fault interactions and seismic hazard. Journal of Geodynamics 29, 459–467.
Scholz, C.H., Dawers, N.H., Yu, J.-Z., Anders, M.H., Cowie, P.A., 1993. Fault growth and fault scaling laws: preliminary results. Journal of Geophysical Research 98, 21951–21961.
Slejko, D., Neri, G., Orozova, I., Renner, G., Wyss, M., 1999. Stress field in Friuli (NE Italy) from fault plane solutions of activity following the 1976 main shock. Bulletin of the Seismological Society of America 89 (4), 1037–1052.
Tari, V., Pamić, J., 1998. Geodynamic evolution of the northern Dinarides and the southern part of the Pannonian Basin. Tectonophysics 297, 269–281.
Vannucci, G., Gasperini, P., 2004. The New Release of the Database of Earthquake Mechanisms of the Mediterranean Area (EMMA Version 2). Annali di Geofisica 47 (Supplement 1), 307–334.
Vermilye, J.M., Scholz, C.H., 1999. Fault propagation and segmentation: insight from the microstructural examination of a small fault. Journal of Structural Geology 21, 1623–1636.

Viola, G., Odonne, F., Mancktelow, N.S., 2004. Analogue modelling of reverse fault reactivation in strike-slip and transpressive regimes: application to the Giudicarie fault system, Italian Eastern Alps. Journal of Structural Geology 36, 401–418.

Vrabec, M., Fodor, L., 2006. Late Cenozoic tectonics of Slovenia: structural styles at the North-eastern corner of the Adriatic microplate. In: Pinter, N. (Ed.), The Adria Microplate: GPS Geodesy, Tectonics and Hazards. NATO Science Series IV, 61. Earth and Environmental Sciences, pp. 151–168.

Weber, J., Vrabec, M., Stopar, B., Pavlovčič Prešeren, P., Dixon, T., 2006. The PIVO 2003 experiment: A GPS study of Istria peninsula and Adria microplate motion, and active tectonics in Slovenia. In: Pinter, N. (Ed.), The Adria Microplate: GPS Geodesy, Tectonics and Hazards. NATO Science Series IV, 61. Earth and Environmental Sciences, pp. 305–320.

Wells, D.L., Coppersmith, K.J., 1994. New empirical relationships among magnitude, rupture length, rupture width, rupture area and surface displacement. Bulletin of Seismological Society of America 84, 974–1002.

Wesnousky, S.G., 2006. Predicting the endpoints of earthquake ruptures. Nature 444, 358–360, doi:10.1038/nature05275.

Zupančič, P., Cecić, I., Gosar, A., Placer, L., Poljak, M., Živčić, M., 2001. The earthquake of 12 April 1998 in the Krn Mountains (Upper Soča valley, Slovenia) and its seismotectonic characteristics. Geologija 44 (1), 169–192.

Živčić, M., 2005. Catalogue of instrumentally located earthquakes in Slovenia 1981–2005, Environmental Agency of the Republic of Slovenia, Seismology and Geology Office, unpublished material.

Živčić, M., Krn-2004 team, 2006. The Krn mountains (Slovenia) M_W 5.2 earthquake: data acquisition and preliminary results. Geophysical Research Abstracts 8, 06439.